Life Sciences in Space Research 46 (2025) 1–9

Contents lists available at ScienceDirect

Life Sciences in Space Research

journal homepage: www.elsevier.com/locate/lssr

Activation of the visual system by space radiation: A novel study on Ca^{2+} signalling in *ex-vivo* rabbit eyes exposed to visible light, X-rays and high-energy protons

I. Borromeo [a,1], A. Mentana [b,*,1], G. Baiocco [b], S. Beninati [a], V. Boretti [c,d], G. Cappadozzi [e], L. Di Fino [f], A. Facoetti [g], L. Lunati [c,d], M. Paci [a], M. Pinto [e], M. Pullia [g], A. Rizzo [h], G. Santi Amantini [c], S. Toma [e,i], L. Narici [c]

[a] *Department of Biology, University of Rome Tor Vergata, Rome, Italy*
[b] *Radiation Biophysics and Radiobiology Laboratory, Department of Physics, University of Pavia, Pavia, Italy*
[c] *Department of Physics, University of Rome Tor Vergata and INFN Sect. Tor Vergata, Rome, Italy*
[d] *Biophysics Department, GSI Helmholtzzentrum für Schwerionenforschung, Darmstadt, Germany, and Technische Universität Darmstadt, Institut für Physik Kondensierter Materie, Darmstadt, Germany*
[e] *National Institute for Metrology of Ionizing Radiation, ENEA - C.R. Casaccia NUClear Department (INMRI), Rome, Italy*
[f] *Italian Space Agency, Rome, Italy*
[g] *CNAO National Center for Oncological Hadrontheraphy, Pavia, Italy*
[h] *Institute of Radioprotection (IRP) - ENEA - C.R. Casaccia, Rome, Italy*
[i] *Faculty of Engineering, University of Cassino and Southern Lazio, Italy*

ARTICLE INFO

Keywords:
Visual system activation
Space radiation
$Ca2^{+}$ signalling

ABSTRACT

Space radiation interactions with the visual system have been the subject of many investigations, starting from astronauts reporting the perception of light flashes (visual illusions in absence of light stimuli). These perceptions have been attributed to single-ion hits, able to induce an electrophysiological response in the eye. Searching for a more general mechanism of radiation interaction with cortical neuronal networks and with sensory systems, a valuable hypothesis is that of the perturbation to calcium (Ca^{2+}) homeostasis.

We here report results on radiation-induced perturbation of Ca^{2+} signalling obtained with an *ex-vivo* whole rabbit eye model. Surgically enucleated eyes (from animals intended for human consumption) were kept in viable conditions and exposed to visible light (varying the duration of the exposure), to kilovoltage X-rays (reference radiation, dose range 10–200 mGy) and to 230 MeV protons (representative of the main component of space radiation, dose range 10–20 mGy). After extraction of the vitreous humor, sample stability and homogeneity in the animal population and organ conditions were verified by measuring the concentration of biogenic polyamines, while eye integrity was tested by measuring the lactate dehydrogenase (LDH) enzymatic activity. The activation of the visual response is attributed to a change in the Ca^{2+} concentration (expressed μg calcium/μg amines) comparing, for each animal, the left eye used as a control and the right eye exposed to light or ionizing radiation. The vitrectomy was conducted immediately after the exposure.

A significant increase in Ca^{2+} concentration was measured after white light exposure with a duration longer than 1 min, with a saturation to a ~150 % relative change for exposure durations of 3 and 5 min. The model was therefore validated for the visual system activation by light, but no increase in Ca^{2+} concentration was found for ionizing radiation exposures in the investigated dose ranges. Only at the highest X-ray dose of 200 mGy, eyes were severely damaged, as demonstrated by the drastic increase in LDH activity. Based on these findings, the limitations of the study are critically discussed, and improvement strategies are suggested, also considering the rapid kinetics of the perturbation that might hinder the measurement of small ionizing radiation-induced transient Ca^{2+} changes.

* Corresponding author.
E-mail address: alice.mentana@unipv.it (A. Mentana).
[1] equally contributing.

https://doi.org/10.1016/j.lssr.2025.03.003
Received 24 October 2024; Received in revised form 30 January 2025; Accepted 11 March 2025
Available online 17 March 2025

1. Introduction

Long-term exposure to ionizing radiation (IR) is one of the biggest challenges to space exploration: a clear understanding of the mechanisms underlying radiation interactions in the human body and the associated biological effects is fundamental to estimate the possible damage, and develop dedicated countermeasures to mitigate health risks (Durante M. and Cucinotta F.A. 2011).

Space radiation interactions with the visual system have been the subject of many investigations during the last decades, since the time of the Apollo missions, when astronauts reported the perception of the so-called phosphenes: visual illusions, in the absence of light stimuli, described as flashes of lights (hereinafter referred to as light flashes, LF). Since then, almost all astronauts have confirmed these perceptions (Pinsky et al., 1974). From the beginning, LF have been attributed to single-ion hits, able to induce an electrophysiological mass response in the retina (Narici, 2010), thus activating the visual system. This mechanism has been investigated with *in-vivo* ground experiments on mice irradiated with bursts of ^{12}C ions (Sannita W. G. 2007; Carozzo S. 2015). Interestingly, perceptions analogous to LF have been experienced by patients undergoing hadron therapy treatments, as more recently reported by several studies conducted on ^{12}C ion therapy patients at GSI (Darmstadt, Germany) (Schardt D. and Krämer M. 2002; Schardt D. 2013) and on proton therapy patients at ICPO (Orsay, France) and at PTRC (Loma Linda, California, USA) (Khan E. 2010; Chuard D. 2016 and Narici L. 2020, respectively). For a review see Narici L. 2024.

The variety of characteristics in LF, e.g. in terms of color and shape, might suggest different underlying mechanisms. Cherenkov radiation produced by the slowing down of relativistic ions in the eye has been indicated as a possible candidate, but it can account for few of the reported LF phenomena, due to specific features of these perceptions (Chuard D. 2016). In general, LF have been attributed to the interaction between IR and ocular structures, mostly directly within the retina. A model proposed by Narici et al. (Narici L. 2009) suggests that IR can activate rhodopsin, giving rise to visual illusions: radiation traversing the eye generates free radicals; the recombination of these with lipids (lipid peroxidation), highly concentrated in photoreceptors located in the retina, is known to produce chemiluminescence with the emission of photons in the visible band (Catalá 2006). The absorption of these photons by the retinal rod outer segment bleaches rhodopsin and therefore starts the phototransduction cascade. The model was tested in vitro using samples of intact bovine retinal rod outer segments (Narici L. 2012; Narici et al., 2013).

However, in addition to processes involving the visual system, different studies seem to point out to a more general mechanism of IR interaction with cortical neuronal networks and sensory systems (Narici L. 2024). This is the case of in vivo experiments with mice (Sannita W. G. 2007; Carozzo S. 2015) and, in particular, of the recent PTRC clinical study on proton therapy (Narici et al., 2020), with patients reporting illusions affecting sensory systems other than visual (auditory, olfactory and gustative) in the course of the treatment.

Looking for a more general mechanism of IR-induced activation of sensory systems, a valuable hypothesis is that of radiation-induced perturbation to calcium (Ca^{2+}) homeostasis. As known, cells can maintain a large concentration gradient between the cytosol (basal Ca^{2+} levels typically ~ 50 nM) and the extracellular space (Ca^{2+} ~ 1.5 mM). Starting from this huge gradient, Ca^{2+} influx across the membrane and Ca^{2+} release from intracellular storage sites may produce large fluctuations in Ca^{2+} concentrations upon stimuli of different kinds (Krizaj D. and Copenhagen D.R. 2002; Alberts B. 2014). The alteration of cytosolic calcium concentration is a signal to activate ion channels and G protein-coupled receptors following an indirect signal transduction. The numerous effects can be visual, or affect muscle contraction, neuronal transmission, cell motility, proliferation and other cellular activities (Clapham D.E. 2007).

In this context, the VISAIR – *VIsual System Activation by Ionizing Radiation* – project, funded by the Italian Space Agency, aimed at continuing the investigation on the IR-induced visual system activation, shedding light on the underlying mechanisms. The project was based on the idea of investigating LF as a "whole-eye" effect, involving, most likely, structures other than the retina only. Radical recombination reported in the chemiluminescence model (Narici L. 2009), Cherenkov emission, as well other direct mechanisms leading to visual effects all fit into this frame. More specifically, the project focused on testing perturbation to Ca^{2+}signalling in the whole eye induced by low doses of a space-relevant radiation quality (high-energy protons), looking for a possible explanation for the activation of the visual system and a link to other radiation-induced sensory system illusions.

Calcium ion homeostasis was therefore studied at the whole organ scale, looking for IR-induced variation of Ca^{2+}concentration in the vitreous humor. The *ex-vivo* whole rabbit eye has been proposed as a new experimental model to be adopted in these kinds of studies. Due to their similarity to human eyes in both structures and dimensions, rabbit eyes are already widely used and recommended as a model to understand human ocular diseases (Qin G. 2022; ARVO, 2025).

To reduce animal testing, rabbits used for this exploratory study were animals intended for human consumption. Eyes were surgically enucleated and maintained in viable conditions. They were then exposed to visible light (varying the duration of the exposure), for viability control and model validation, testing the activation of the visual response. Once the model response to light was validated, eyes were exposed to X-rays and high-energy protons to explore the possible IR-induced activation. As common in radiobiological studies, X-rays were chosen as a reference radiation quality, while protons were chosen as representing the most abundant component of the space radiation environment. For both radiation qualities, dose-response curves were measured: dose values were chosen focusing on the low-dose range relevant for space applications, and taking care of the possible induction of damage to the eye as a limiting condition (Narici et al., 2013). In all experiments, both eyes from the same animal were used: one was exposed and the other was kept in the dark and used as a reference to measure basal quantities, thus controlling inter-animal variability when measuring the individual response. The new model required a preliminary definition of the experimental strategy for the stabilization of the samples. An initial characterization, to evaluate both the homogeneity of the samples from the rabbit population (biogenic polyamines) and the cellular viability of the organs (activity of lactate dehydrogenase, LDH), was also necessary. The experimental approach included the planning of the radiation exposure procedures at different facilities (Mentana A. 2020) and the statistical data processing.

In this work, we present and critically discuss the details and the results of the experimental measurements performed with the new *ex-vivo* rabbit eye model, measuring perturbation to Ca^{2+}signalling to test the activation of the visual system by space-relevant doses of ionizing radiation.

2. Material and methods

2.1. Reagents and chemicals

All reagents were analytical grade or equivalent and purchased from Merck KGaA, Darmstadt, Germany. All solutions were freshly prepared with ultrapure water, generated by Elix® 5 Water Purification Systems (Millipore, Billerica, MA, USA) water deionizer.

2.2. Organ culture of rabbit eyes

Rabbit eyes were collected from animals intended for human consumption within a maximal amount of time of 24 h elapsed from slaughtering. Slaughtered rabbits were all within 10 to 13 weeks old, weighting from 2 to 3 kg. The enucleated rabbit eye was removed and soaked for 10 s in 96 % ethanol, washed with sterile phosphate buffer

saline (PBS, pH 7) and placed in a Falcon tube containing 10 mL of buffer solution made with 9.3 mL of sterile PBS (without Ca^{2+}), 0.5 mL of penicillin 100 U/mL and streptomycin 100 µg/mL and 0.2 mL of 1 M Hepes. The organs were stored at +4 °C in the dark, until exposure to light or ionizing radiation. The vitrectomy was conducted immediately after the exposure (in the case of proton exposures, a waiting time of the order of a few minutes was necessary to verify sample activation before handling) at room temperature (RT).

2.3. Vitrectomy and sample preparation

The rabbit eyes were placed on the ocular dissection chamber: the sclera was incised 5 mm transversely using a sterile scalpel or scissors. Vitreous humor was collected utilizing 1 mL insulin syringe. Representative pictures of the organ culture and vitrectomy procedure are shown in Fig. 1. The collected vitreous humor was transferred in an Eppendorf tube. Due to the high viscosity of the sample, a dilution of pure vitreous humor was carried out using PBS (pH 7). The final concentration of the vitreous samples was calibrated to 20 mg/mL (dilution factor, DF = 50). Pure vitreous and diluted samples were stored at −20 °C until the tests were performed.

2.4. Determination of total biogenic amine levels

Total amine levels were determined according to Grewal (Grewal I.K. 2020) with major modifications. All pure vitreous samples were thawed at RT and vortexed for one minute to make a homogeneous solution. A fresh solution of dansyl chloride (Dns-Cl) (6 mg/mL acetone) was prepared and kept in the dark until use. 20 mg of pure vitreous humor were dissolved in 2.5 mL of double distilled water; 2.5 mL of Dns-Cl solution and 0.1 mL of 100 % methanol were added to the samples. Vitreous humor samples were kept in the dark for 2 h at RT. At the end of incubation time, 20 mL of double distilled water were added to the samples, and samples were vortexed for 30 s.

The amine concentration was obtained according to a calibration curve, made with known final concentrations of a putrescine solution (20, 40, 60, 80, 100, 120, 140, 160, and 180 µg/mL) ($y = 0.0451x + 0.0264$; $R^2 = 0.991$), with an initial concentration of 200 µg/mL, dissolved in double distilled water. The absorbance was read at $\lambda = 369$ nm with a spectrophotometer (VARIAN Cary 50 Bio, Santa Clara, CA, USA), using water as a blank. Results were expressed as µg amines/mg vitreous humor.

2.5. Determination of calcium levels

Calcium concentration was determined using the Calcium Assay Colorimetric Kit (Abcam, Cambridge, UK— ab272527; www.abcam.com/ab272527, accessed March 30, 2024) and a multimode microplate reader set to 612 nm (Spark® Multimode Microplate Reader—Tecan, Switzerland). The calcium test was performed with 5 µL (DF = 41) of the diluted vitreous sample. The detection range of kit was 20 - 5000 µM; the results were expressed as the ratio of µg calcium/µg amines. Raw data on µg calcium/mg vitreous concentrations are reported in Table 1S in Supplementary Material.

2.6. Lactate dehydrogenases (LDH) activity assay

A LDH activity assay kit (Sigma-Aldrich – MAK066, https://www.sigmaaldrich.com/IT/it/product/sigma/mak066, detection range: 2.5 - 12.5 nmole/well, accessed April 16, 2024) was used to study enzyme activity. The assay was performed with 50 µL of the diluted vitreous sample. Absorbance values were measured using a multimode microplate reader at 450 nm (Spark® Multimode Microplate Reader—Tecan, Switzerland). LDH activity was expressed as enzymatic units/mL solution.

2.7. Exposure protocols

Exposures to white light were performed at the Laboratory of Cell Biochemistry and Experimental Oncology, Department of Biology, University of Rome Tor Vergata, Italy. A dedicated setup was built with a commercial lamp and a holder for the transparent Falcon tube containing the eye. The tube was kept in the dark for 24 h before the experiment and then exposed for 1, 3 and 5 min to a white light beam (10,000–11,000 LUX) using a SILAMP E27 RGB LED lamp with a power of 5 W that provides a light intensity of 450 lumens at an illumination angle of 120°.

For all IR exposures (both X-rays and proton beam), the Falcon tubes containing the rabbit eyes were darkened with a black varnish and also covered with an aluminum foil, which was removed only during irradiation. This was done to prevent simultaneous light and IR exposure.

X-ray exposures were performed at the National Institute for Metrology of Ionizing Radiation, ENEA - C.R. Casaccia (INMRI), Italy. Dosimetry was realised using the primary standard of absorbed dose to water of Italy, a graphite calorimeter in a water phantom (Pinto M. 2016), a unique system ensuring reduced uncertainty if compared to measurement methods based on air kerma and its subsequent conversion to dose to water (e.g. based on a dosimetry protocol or code of practice). Eyes were exposed with X-rays generated by an X-ray tube under reference conditions (248.6 – 249.5 kV, 0.5 mA – 10.3 mA, expected LET~2 keV/µm in water), obtaining dose rates in the range of 0.10 – 2.91 mGy/s and adjusting the exposure time to obtain nominal doses of 10, 25, 50 and 200 mGy. The duration of irradiation could vary from 50 to a maximum of 100 s. For the irradiation, the Falcon tubes were positioned in a holder and their lower part was immersed in a water phantom to ensure homogeneity of the dose in the organ. The X-ray field area was large enough to cover the bottom of the tube containing the eye. The dose-depth curve in water was measured for all

Fig. 1. Representative photos of the organ culture method and its manipulation for the preparation of the vitreous humor sample: culture of the rabbit eye in a Falcon tube (1a) and organ positioned in the ocular dissection chamber (1b); incision of the sclera for vitrectomy (1c) and sampling of the vitreous humor using a 1 mL syringe (1d). To limit the exposure to ambient light during vitrectomy, the eye was placed in the dissection chamber with the pupil facing downwards.

exposures using an ionization chamber. Considering the uncertainty in the eye positioning and the average size of the eye, the average dose imparted to the whole eye is estimated to be subject to an uncertainty of the order of 2 %.

Proton exposures were performed at the National Center for Oncological Hadrontherapy, CNAO – Pavia, Italy. Eyes were exposed to 230 MeV protons (LET~0.4keV/μm in water) and the exposure time was adapted based on the number of protons per spill and number of spills per second to obtain nominal doses of 10 and 20 mGy. The duration of the exposure was of a few seconds for all conditions. Falcon tubes were placed in a holder positioned along the beam line, protons were delivered covering the bottom of the tube containing the eye with a 24×24 spot field, with a 3 mm spacing between two adjacent spots. Irradiations were performed in air. No significant dose inhomogeneity is expected in the whole organ: Monte Carlo simulations predicted a dose variation with respect to the average dose value of the order of 2 %, considering the uncertainty in the eye positioning and the average size of the eye.

Representative photos of experimental setups for IR exposures at the INMRI-ENEA and CNAO facilities are shown in Fig. 2.

2.8. Experimental strategy

To test the perturbation of Ca^{2+} signalling, we quantified the Ca^{2+}concentration in vitreous humor collected after vitrectomy of the whole eye exposed to white light, X-rays and protons. To overcome possible inhomogeneity of the vitrous humor, Ca^{2+}concentration values were expressed as Ca^{2+}/amine ratio, measured in μg Ca2+/μg amines, thus requiring prior quantification of amine concentration (expressed in μg amines/mg vitreous) and a series of protocol steps including sample dilution, as above described. LDH activity was also measured in the same samples.

For each rabbit included in the study, one eye (left) was exposed to light/IR and the other one (right) was kept in the dark and used as control, providing the basal level of all measured quantities. This experimental strategy was conceived to pool in a single analysis the results obtained from different animals, at least partially overcoming the inter-individual variability.

Fig. 2. Representative photos of the experimental setups for IR eye exposures Top: two different views of the setup for X-ray exposures in the INMRI ENEA premises, with the darkened Falcon tube positioned with its lower edge in the water phantom. Bottom: setup for proton exposures in the CNAO, with an empty transparent Falcon tube positioned along the proton beam line.

In a homogeneous population, basal biogenic amine concentration values are not expected to vary significantly among different animals. For the same animal, μg amines/mg vitreous humor values are not expected to vary between the control and the exposed eye, as amine levels are not affected by light or IR exposure.

In case of activation upon exposure to light or IR, a change in the Ca^{2+}/amines ratio is expected instead when comparing the exposed eye to the control one of the same animal. The entity of the change, if present, might also be affected by inter-individual variability, both because of different basal levels or because of a different response to the same stimulus. Data were therefore analyzed with different strategies: both pooling the results of the different animals together (for all measured quantities), and quantifying the relative change in Ca^{2+}concentrations when comparing the exposed eye and the control eye for each animal.

All measured quantities were examined as a function of white light exposure time (1, 3 and 5 min), X-ray dose (10, 25, 50 and 200 mGy) and proton dose (10 and 20 mGy). Three and five rabbits per exposure time/dose have been used in the white light and IR tests, respectively ($n = 3$ or $n = 5$). For every single eye, two (white light test) or six (IR tests) samples of the vitreous body were taken and then analyzed individually, hence resulting in two/six values of all quantities (amine concentration, Ca^{2+} concentration, and LDH activity). Such values were averaged for the single exposed and control eye for each animal. Average values for the single exposed and control eye were used for the calculation of relative change values (Ca^{2+} concentration) for each animal. The mean values for all exposed and control eyes of all animals were further averaged. Relative values for the relative Ca^{2+} concentration change for all animals were also averaged, and errors propagated.

2.9. Statistical analysis

Statistical significance was evaluated by the two-tailed *t*-test: * $p < 0.05$, ** $p < 0.01$, *** $p < 0.005$. The *t*-test was used for the Ca^{2+}/amine concentration comparisons of exposed vs. control eyes in each single time/dose condition. Analogously, the *t*-test was used to evaluate the difference in LHD activity of exposed vs. control eyes for light, X-ray and proton exposures.

The statistical significance evaluation has been also performed for the Ca^{2+}/amine concentration relative increase. In this case, *t*-test was used for the relative change comparison with respect to the baseline.

3. Results

3.1. Measurement of biogenic amine concentration

The results of the biogenic amine concentration measurements are shown pooled for all animals in the upper panels of Figs. 3–5, for exposure to white light, X-rays and protons respectively. In the graphs, each box represents the amine concentration values (expressed as μg amines/mg vitreous) averaged for all eyes considered for a given condition. Details on the boxplot representation can be found in the caption. For white light (Fig. 3), the amine concentration is shown for the three selected exposure times: 1, 3 and 5 min; for X-rays (Fig. 4) and protons (Fig. 5), the amine concentration is shown for the tested dose values (10, 25, 50 and 200 mGy for X-rays and 10 and 20 mGy for protons, respectively). The blue boxes always refer to the control eyes, while the other colors indicate the exposed eyes.

Biogenic amine concentration is not affected by light or IR exposure, as expected. Variations between different animals are reflected in the scatter of the measured amine concentration values for eyes in the same condition. Overall, this scatter was considered acceptable for the inclusion of all animals in the study, indicating the selection of a homogeneous population and organ conditions. Differences in the absolute values of amine concentrations among the three different datasets of Figs. 3–5 could reflect variations in environmental conditions (e.g.

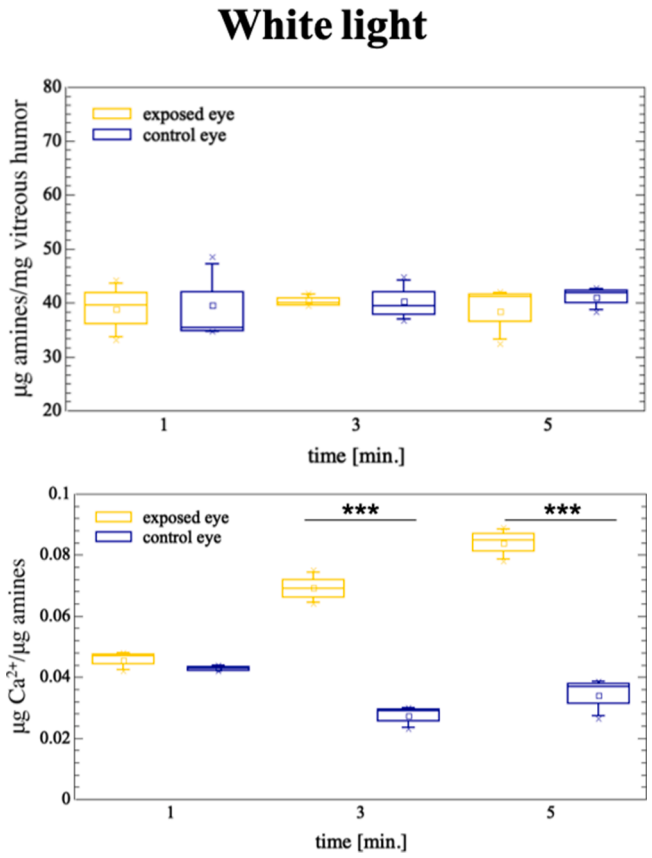

Fig. 3. Biogenic amine (upper panel, in µg amines/mg vitreous) and calcium (lower panel, in µg Ca^{2+}/µg amines) concentrations in eyes exposed to white light ("exposed", left eyes for all animals) and unexposed eyes ("control", right eyes for all animals). Three different exposure times to white light have been examined: 1, 3 and 5 min, each with $n = 3$ animals and two vitreous samples per eye, whose results were averaged. The box contains the middle 50 % of the average values, from the 25th percentile (bottom of the box) to the 75th percentile (top of the box). The square and the line within the box are the mean and median respectively. Whiskers are drawn to the 5th and up to the 95th percentiles and the "x" symbols indicate the smallest and largest values. Blue boxes always refer to the control eyes and yellow boxes to the exposed ones. Statistical significance was evaluated by the two-tailed *t*-test for the comparison of exposed vs. control eyes in each single condition: * $p < 0.05$, ** $p < 0.01$, *** $p < 0.005$.

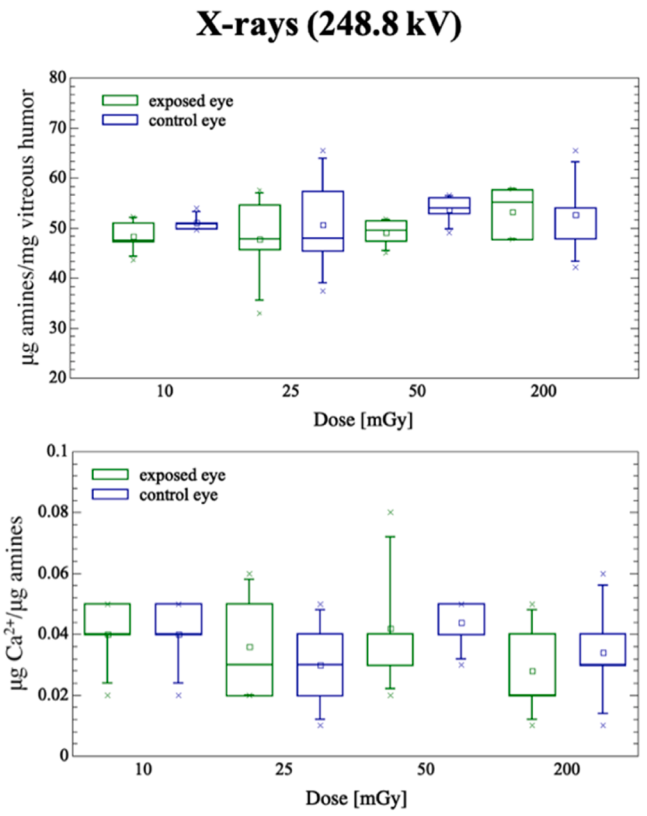

Fig. 4. *Biogenic amine (upper panel, in µg amines/mg vitreous) and calcium concentration (lower panel, in µg Ca^{2+}/µg amines) in eyes exposed to X-rays ("exposed", left eyes for all animals) and non-exposed eyes ("control", right eyes for all animals). Four different doses have been examined: 10, 25, 50 and 200 mGy, each with $n = 5$ animals and six vitreous samples per eye, whose results were averaged. The box contains the middle 50 % of the average values, from the 25th percentile (bottom of the box) to the 75th percentile (top of the box). The square and the line inside the box are the mean and median, respectively. Whiskers are drawn to the 5th and up to the 95th percentiles and the "x" symbols indicate the smallest and largest values. Blue boxes always refer to the control eyes and green boxes to the exposed ones.* Statistical significance was evaluated by the two-tailed *t*-test for the comparison of exposed vs. control eyes in each single condition: * $p < 0.05$, ** $p < 0.01$, *** $p < 0.005$.

temperature, humidity etc.), impacting on the calibration curve, or indicate some extent of protein degradation leading to amine formation when eyes are subject to longer handling (i.e. for the X-ray and proton exposures at external facilities). However, amine absolute values do not impact the conclusion of the study, as later discussed, and no significant biological degradation is observed in control eyes for all experiments (see results for LDH measurements in Section 3.3).

3.2. Measurement of Ca^{2+} concentration

The results of calcium concentration measurements, expressed as Ca^{2+}/amine ratio, are shown pooled for all animals in the bottom panels of Figs. 3–5, for exposure to white light, X-rays and protons, respectively. Details on the boxplot representation can be found in the caption. For white light (Fig. 3), Ca^{2+} concentration is shown for the three selected exposure times: 1, 3 and 5 min; for X-rays (Fig. 4) and protons (Fig. 5), Ca^{2+} concentration is shown for the tested dose values (10, 25, 50 and 200 mGy for X-rays and 10 and 20 mGy for protons). The blue boxes always refer to the control eyes, while the other colors indicate the exposed eyes.

Comparing the measurements of calcium concentration between the exposed and control eyes in each condition, a significant difference is observed for white light exposure with a duration of 3 and 5 min. No significant difference is observed for exposures to different IR doses, neither for X-ray nor proton irradiation. In control eyes, the scatter in the measured values may reflect inter-animal variability in both basal amine levels (used to calculate the Ca^{2+}/amine ratio) and basal Ca^{2+} concentrations. In exposed eyes, such basal variability could add to a different sensitivity, due to inter-animal variability in the response to the exposure. Therefore, the scatter in measured Ca^{2+} values is overall larger than for the quantification of amine. For the sake of completeness, data on calcium concentrations in the humor vitreous (µg Ca^{2+}/mg vitreous) are also reported as Supplementary Material.

A different analysis of the same dataset from Figs. 3–5 is shown in Fig. 6, where the values for the relative change in Ca^{2+} concentration in the exposed eye with respect to the control eye are calculated for each animal:

$$Relative\ change = \frac{Ca^{2+}\ (exposed\ eye)\ -\ Ca^{2+}\ (control\ eye)}{Ca^{2+}\ (control\ eye)}.$$

The relative change value is close to zero when the exposure does not change the Ca^{2+} concentration, while positive values indicate an increase in Ca^{2+} concentration: for example, a value of 1 means that a

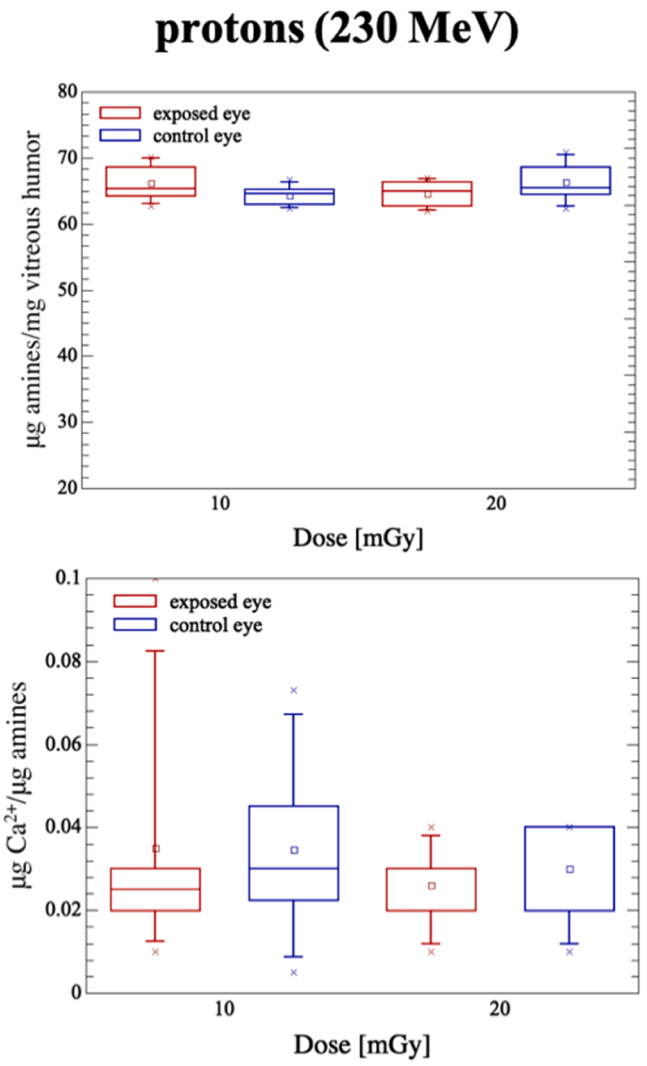

Fig. 5. *Biogenic amine (upper panel, in* µg *amines/*mg *vitreous) and calcium (lower panel, in µg Ca^{2+}/µg amines) concentrations in eyes exposed to protons ("exposed", left eyes for all animals) and unexposed eyes ("control", right eyes for all animals). Two different doses have been examined: 10 and 20 mGy, each with n = 5 animals and six vitreous samples per eye, whose results were averaged. The box contains the middle 50 % of the average values, from the 25th percentile (bottom of the box) to the 75th percentile (top of the box). The square and the line inside the box are the mean and median, respectively. Whiskers are drawn to the 5th and up to the 95th percentiles and the "x" symbols indicate the smallest and largest values. Blue boxes always refer to the control eyes and red boxes to the exposed ones.* Statistical significance was evaluated by the two-tailed *t*-test for the comparison of exposed vs. control eyes in each single condition: * $p < 0.05$, ** $p < 0.01$, *** $p < 0.005$.

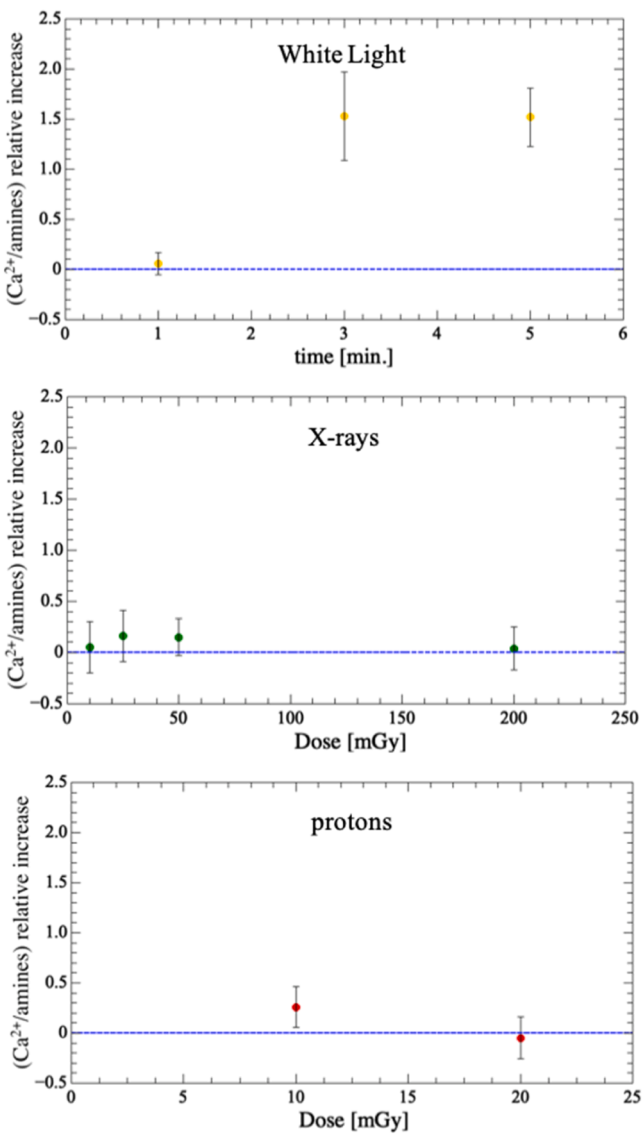

Fig. 6. *Relative increase in calcium concentration in the exposed rabbit eye with respect to the control one of the same animal as a function of exposure time to white light (upper panel), X-ray dose (middle panel) and proton dose (lower panel). The relative increase in (µg Ca^{2+}/µg amines) is calculated as the absolute increase,* i.e. *the difference between (µg Ca^{2+}/µg amines) in the exposed eye and the control eye, divided by (µg Ca^{2+}/µg amines) in the control eye. The error bars were calculated by propagating the* uncertainties, using the standard deviations of the experimental measurements.

double concentration was measured in the exposed eye with respect to the control eye (relative increase of 100 %). The results for relative change values are then pooled together for all animals considered for a given condition. Such analysis was performed for exposure to white light (Fig. 6, top panel), X-rays (Fig. 6, middle panel) and protons (Fig. 6, lower panel). Each point in the graphs represents the average relative change for all animals under the same exposure condition. Error bars have been calculated using error propagation laws, starting from the standard deviations of the Ca^{2+} concentration measurements.

This analysis confirms what was previously observed in Figs. 3–5, but allows a proper quantification of the change in Ca^{2+} concentration, at least partially accounting for inter-animal variability: the increase in calcium concentration with exposure time is clearly visible in the white light test (Fig. 6, upper panel) for exposure durations longer than 1 min. In particular, for eyes exposed to white light for 3 min, the relative increase is about 150 %, and a similar value is obtained for 5-minute exposures. Looking at the trend in the data, a saturation of Ca^{2+} signalling activation can be guessed between 1 and 3 min of exposure.

These conclusions have been further confirmed by the significance analysis performed as described in Section 2.9: the relative change in Ca^{2+}/amine concentration is significant for 3 (*) and 5 (***) minutes of exposure to white light.

In contrast, the two tests performed with IR show no radiation-induced effect on calcium concentration in the eye, at least not in the investigated dose-range: for both X-ray irradiations (Fig. 6, middle panel) and proton irradiations (Fig. 6, lower panel), the relative change values are always compatible with zero considering the associated uncertainties. A value higher than zero can be observed for the lowest proton dose (10 mGy), which, however, is not statistically significant.

3.3. LDH activity measurements

The results of the LDH activity measurements are shown pooled for all animals in Fig. 7, for exposure to white light (upper panel), X-rays (middle panel) and protons (lower panel). Details on the boxplot representation are given in the figure caption. LDH activity is not altered when comparing results for exposed vs. control eyes after white light or proton exposures, but a trend of increasing LDH activity is observed after exposure to increasing doses of X-rays, statistically significant from 50 mGy, with a drastic increase at the highest dose of 200 mGy.

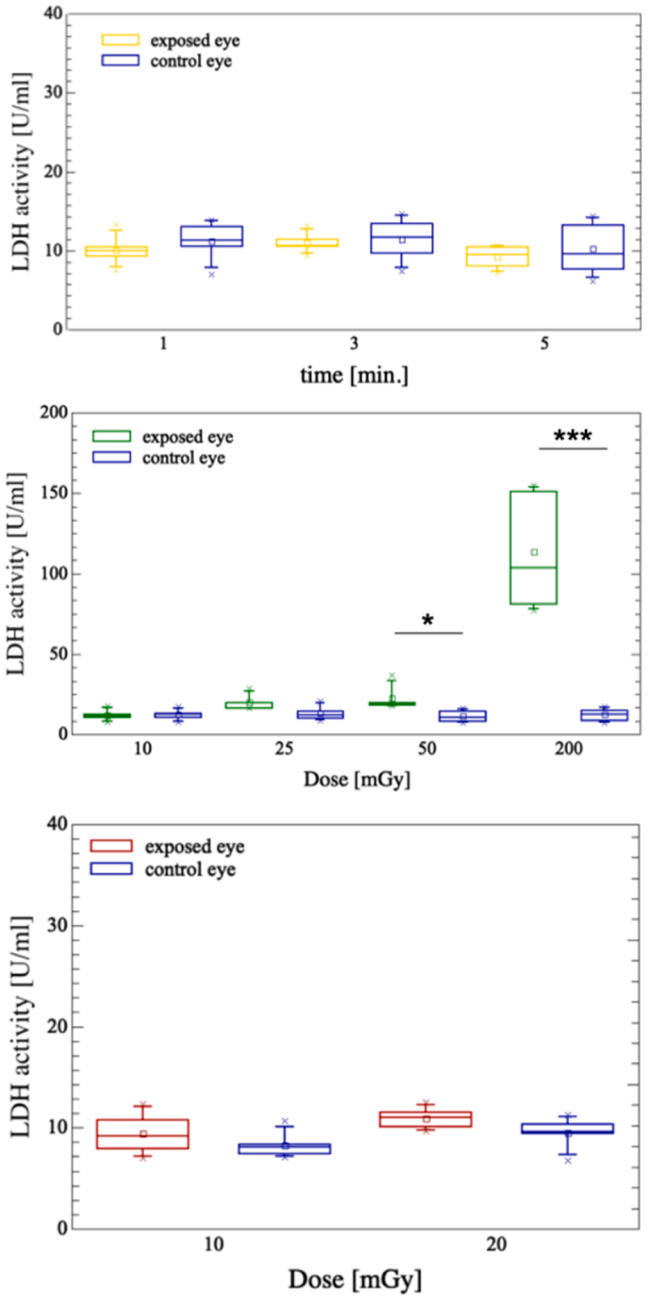

Fig. 7. *LDH activity measured in exposed eyes ("exposed", left eyes for all animals) and unexposed eyes ("control", right eyes for all animals) for all animals under the tested exposure conditions: top panel, as a function of exposure time (1, 3 and 5 min) to white light; middle panel, as a function of dose (10, 25, 100 and 200 mGy) for X-ray; bottom panel, as a function of dose (10 and 20 mGy) for protons. The box contains the middle 50 % of the average values, from the 25th percentile (bottom of the box) to the 75th percentile (top of the box). The square and the line inside the box are the mean and median, respectively. Whiskers are drawn to the 5th and up to 95th percentiles and the "x" symbols indicate the smallest and largest values. Blue boxes always refer to the control eyes and yellow/green/red boxes to the exposed eyes.* Statistical significance was evaluated by the two-tailed *t*-test for the comparison of exposed vs. control eyes in each single condition: * $p < 0.05$, ** $p < 0.01$, *** $p < 0.005$.

4. Discussion

In the framework of the VISAIR project, funded by the Italian Space Agency, we performed an experimental study to verify whether space-relevant doses of ionizing radiation can activate Ca^{2+} signalling in the whole *ex vivo* rabbit eye, kept viable after enucleation. The rabbit eye was chosen because of its well-known similarity, in size and physiology, to the human one. Animals involved in the study were intended for human consumption. As a general approach, for each single rabbit, we considered both eyes: the first one (left) was exposed to radiation, and the second one (right) was kept in the dark and used as a reference/control. We selected as biological markers the biogenic amine concentration in the vitreous humor, to evaluate the sample homogeneity and organ conditions, and the activity of lactate dehydrogenase (LDH), to assess the sample integrity. The Ca^{2+} concentration was determined as Ca^{2+}/amine ratio in the vitreous humor, collected via vitrectomy right after exposures.

To our knowledge, such an experimental model has never been used in previous radiation biology studies to investigate the visual system response to radiative stimuli. Therefore, a preliminary test was necessary to demonstrate that Ca^{2+} signalling is activated after exposure to white light. Data reported in the upper panel of Fig. 6 (relative increase in calcium concentration in the exposed eye compared to the control one of the same rabbit) show that Ca^{2+} concentration in the vitreous body is significantly altered (increased by a factor 1.5) by white light for exposure durations longer than 1 min. Moreover, a possible signal saturation can be guessed, with Ca^{2+} concentration reaching a plateau for longer exposure durations. Previous studies on Ca^{2+} release response in toad excised retina under illumination with white light (Gold G.H. and Korenbrot J.I. 1980) also reported a transient light-induced increase in extracellular calcium concentration.

Building on these results, rabbit eyes were then exposed to different doses of X-rays (248.6 – 249.5 kV), as a reference radiation quality, and high-energy protons (230 MeV), as representative of the most abundant component of the space radiation environment. In both these two sets of experiments, no response of the system to IR is observed in terms of Ca^{2+} concentration: Ca^{2+} signaling seems not to be affected by IR exposure in the explored dose range, 10 to 200 mGy for X-rays and 10 to 20 mGy for protons. This is shown by data reported in the middle and lower panels of Fig. 6, for X-rays and protons respectively. Only the lowest tested proton dose (10 mGy) appears to cause a small relative change in Ca^{2+} concentration (lower panel) but the result is not statistically significant.

LDH activity measurements (see Fig. 7) show that the biological degradation of the eye increases for increasing X-ray doses, up to a high damage level in eyes exposed to the maximal dose of 200 mGy. Such a high dose value can indeed be expected to cause degradation of the eye (Narici et al., 2013), and this condition was chosen as a positive control. LDH activity was instead found unaffected by white light as well as proton exposure up to 20 mGy.

Of interest, a previous study on the response to high dose (5 Gy) X-ray irradiations in rat lenses (Kandaz M. 2009), conducted on 12 animals, has shown an increase of Ca^{2+} release by almost a factor 2, comparing irradiated and control eyes (from 11.79 to 19.47 mg/dL). However, the measurement of malondialdehyde (MDA) levels in lenses indicated that severe oxidative damage occurs in irradiated eyes. In this work, much lower doses have been explored as relevant for the space radiation scenario, with the idea of maintaining exposure levels below the possible damage threshold.

A major difficulty in this study is related to inter-individual variability in both basal quantities (biogenic amine and Ca^{2+}

concentration), measured in unexposed eyes, and in the possibly different sensitivity levels of different animals to the same stimulus, which might lead to a different activation of Ca^{2+} signalling. To partially overcome this limitation, as described in the Material and Methods section, for each animal one eye was exposed to light/IR and the other one was kept in the dark and used as control. Collected data have then been analyzed both pooling together results for the eyes of different animals for a specific condition (Figs. 3–5), and quantifying the relative change of Ca^{2+} concentration by comparing, for each animal, the exposed and the control eye (Fig. 6). The scatter observed in absolute values of amine concentration for different animals indicates that animals included in the study belong to a rather homogeneous population. The scatter in the data is higher for Ca^{2+} concentration values, both because these are expressed as ratio to amine levels, and, in case of exposure to light or IR, also because of the possibly different sensitivity in the response. Care is needed therefore when interpreting average values of Ca^{2+} concentration as shown in Figs. 3–5, and proper quantification of the entity of any light- or IR-induced effect can be concluded only by looking at the relative Ca^{2+} concentration change, shown in Fig. 6. As an example of the gain in sensitivity of this procedure, the small effect induced by the lowest 10 mGy proton dose, though not statistically significant, cannot be observed when looking at data pooled all together.

Another limitation of the exploratory study is the relatively small number of animals (n = 2 to 5 for white light and IR exposures, respectively). This remains dictated by practical reasons, such as the need to perform the vitrectomy right after the exposure, thus limiting the length of a single experiment, and the contemporary availability of rabbits with the same known origin. Of note, the use of rabbits farmed for meat consumption meets the requirement of reducing animal experimentation.

Another important factor affecting the results of this study might be the transient nature of the perturbation to Ca^{2+} signalling. In the previously mentioned study by (Gold G.H. and Korenbrot J.I. 1980), the increase in Ca^{2+} release in toad excised retina after exposure to white light was indeed found to have a duration of the order of ~10 s. In our experimental setup, the handling time of the organ after irradiation, including the vitrectomy procedure, is necessarily of the order of a few minutes. In compliance with radiation protection requirements, an additional waiting (of the same order of magnitude) was necessary to verify sample activation before handling eyes irradiated with high-energy protons. For these reasons, in the early stages of our study, the kinetics of the Ca^{2+} signal after exposing rabbit eyes to white light was also tested. In our conditions, the Ca^{2+} signal induced by light exposure was found to be clearly measurable 2 h after the exposure. Based on this result, we expected that, if proton exposures had induced any alteration of the Ca^{2+} signalling, this would have been measurable even after the unavoidable waiting time to collect eyes and perform the vitrectomy. However, as the functions of the eye have been evolutionarily optimized for the response to visible light, IR-induced effects might indeed be less amplified and more quickly attenuated. If the IR-induced effect has a lower intensity and a transient nature with a much more rapid kinetics, part of (or all) the signal can be lost already after few minutes. This tentative hypothesis could explain why no perturbation to Ca^{2+} signalling has been observed after IR exposure, but remains to be verified further developing the experimental strategy adopted in this work.

5. Conclusions

Radiation-induced perturbation of calcium (Ca^{2+}) homeostasis in the eye is proposed as a mechanism underling the activation of the visual system by space radiation (as in the astronauts' perception of light flashes), as well as of other sensory systems (with other sensory illusions being reported by hadrontherapy patients). To investigate this mechanism, a new experimental *ex-vivo* whole rabbit eye model has been validated in terms of its response to light stimuli, which is measured as an increase of Ca^{2+} concentration in the vitreous humor. No activation of the visual system through a change in Ca^{2+} concentration could be detected instead when exposing eyes to X-rays (248.6 – 249.5 kV) in the dose range 10 – 200 mGy and to 230 MeV protons in the space-relevant dose range 10 – 20 mGy. A significant biological degradation (measured in terms of LDH activity) was found after exposure to X-ray doses higher than 50 mGy.

Overall, the outcome of this pilot work sets the basis for further investigations, based on a whole rabbit eye approach, of the visual system activation by different radiation qualities. In particular, low-dose exposures to high-energy protons have been first explored as representative of the space radiation environment. The selection of a homogeneous animal population, potentially reducing the inter-individual variability, the increase in the number of animals involved and, importantly, a much faster manipulation of the sample after irradiation (i.e. quenching by a cryogenic device) could facilitate the measurement of a possible small transient IR-induced relative change in the Ca^{2+} concentration in the vitreous humor. Advanced techniques to efficiently monitor fast Ca^{2+} concentration change in biological systems (e.g. Power A.S. 2025) could also be used to investigate visual system activation by IR, also with the attractive perspective of developing real-time sensors (Zou J. 2007; Valiente-Gabioud A.A. 2023), but these require significant development to be adapted to our experimental model and will need to be addressed in future studies.

CRediT authorship contribution statement

I. Borromeo: Writing – review & editing, Writing – original draft, Investigation, Data curation. **A. Mentana:** Writing – review & editing, Writing – original draft, Investigation, Formal analysis, Data curation. **G. Baiocco:** Writing – review & editing, Writing – original draft, Supervision, Project administration, Investigation, Formal analysis, Conceptualization. **S. Beninati:** Writing – review & editing, Supervision, Project administration, Methodology, Data curation, Conceptualization. **V. Boretti:** Writing – review & editing, Investigation. **G. Cappadozzi:** Writing – review & editing, Investigation. **L. Di Fino:** Writing – review & editing, Investigation. **A. Facoetti:** Writing – review & editing, Investigation. **L. Lunati:** Writing – review & editing, Investigation. **M. Paci:** Writing – review & editing, Supervision, Investigation, Conceptualization. **M. Pinto:** Writing – review & editing, Investigation. **M. Pullia:** Writing – review & editing, Investigation. **A. Rizzo:** Writing – review & editing, Investigation. **G. Santi Amantini:** Writing – review & editing, Investigation. **S. Toma:** Writing – review & editing, Investigation. **L. Narici:** Writing – review & editing, Supervision, Project administration, Investigation, Funding acquisition, Conceptualization.

Declaration of competing interest

The authors declare that they have no known competing financial interests or personal relationships that could have appeared to influence the work reported in this paper.

Funding

The study was funded by the Italian Space Agency, contract n. 2018–17-U.O, Project: VISAIR – *VIsual System Activation by Ionizing Radiation*.

Supplementary materials

Supplementary material associated with this article can be found, in the online version, at doi:10.1016/j.lssr.2025.03.003.

References

ARVO, 2025. Reccomendation of ARVO Foundation For Eye research, 5515 Security lane, Suite 500. Rockville Maryland, p. 20852.

Alberts, B., 2014. In: Norton, W.W. (Ed.), Essential Cell Biology, 4th ed. Company. https://doi.org/10.1201/9781315815015.

Carozzo, S., Ball, S.L., Narici, L., Schardt, D., Sannita, W.G., 2015. Interaction of 12C ions with the mouse retinal response to light. Neurosci. Lett. 598. https://doi.org/10.1016/j.neulet.2015.04.048.

Catalá, A., 2006. An overview of lipid peroxidation with emphasis in outer segments of photoreceptors and the chemiluminescence assay. Int. J. Biochem. Cell Biol 38, 9. https://doi.org/10.1016/j.biocel.2006.02.010.

Chuard, D., Anthonipillai, V., Dendale, R., Nauraye, C., Khan, E., Mabit, C., De Marzi, L., Narici, L., 2016. Mechanisms of phosphene generation in ocular proton therapy as related to space radiation exposure. Life Sci. Space Res. 10. https://doi.org/10.1016/j.lssr.2016.06.002.

Clapham, D.E., 2007. Calcium signaling. Cell 131, 6. https://doi.org/10.1016/j.cell.2007.11.028.

Durante, M., Cucinotta, F.A., 2011. Physical basis of radiation protection in space travel. Rev. Mod. Phys. 83, 1245. https://doi.org/10.1103/RevModPhys.83.1245.

Gold, G.H., Korenbrot, J.I., 1980. Light-induced calcium release by intact retinal rods. Proc. Natl. Acad. Sci. U.S.A. 77 (9). https://doi.org/10.1073/pnas.77.9.5557.

Grewal, I.K., Singh, S., Arora, S., Sharma, N., 2020. Development and validation of UV-spectrophotometer analytical method of eflornithine hydrochloride. Plant. Arch. 20 (1).

Kandaz, M., Ertekin, M.V., Erdemci, B., Kızıltunç, A., Koçer, İ., Özmen, H.K., Aktan, M.I., Beşe, A.V., 2009. The effects of zinc sulfate on the levels of some elements and oxidative stress occurring in lenses of rats exposed to total cranium radiotherapy. Euras. J. Med. 41 (2).

Khan, E., Maréchal, F., Dendale, R., Mabit, C., Calugaru, V., Desjardin, L., Narici, L., 2010. Anomalous phosphenes in ocular protontherapy. Adv. Space Res. 45, 7. https://doi.org/10.1016/j.asr.2009.11.021.

Krizaj, D., Copenhagen, D.R., 2002. Calcium regulation in photoreceptors. Front. Biosci. 7. https://doi.org/10.2741/A896.

Mentana, A., Baiocco, G., Guardamagna, I., Lonati, L., Ottolenghi, A., Beninati, A., Borromeo, I., Di Fino, L., Paci, M., Romoli, G., Sannita, W.G., Narici, L., 2020. Modelling the irradiation setup for whole rabbit eye exposures. Nuovo Cimento 43. https://doi.org/10.1393/ncc/i2020-20134-0. C.

Narici, L., 2010. Heavy ions light flashes and brain functions: recent observations at accelerators and in spaceflight. New J. Phys. 10. https://doi.org/10.1088/1367-2630/10/7/075010.

Narici, L., De Martino, A., Brunetti, V., Rinaldi, A., Sannita, W.G., Paci, M., 2009. Radicals excess in the retina: a model for light flashes in space. Radiat. Meas. 44. https://doi.org/10.1016/j.radmeas.2009.01.005.

Narici, L., Paci, M., Brunetti, V., Rinaldi, A., Sannita, W.G., De Martino, A., 2012. Bovine rod rhodopsin. 1. Bleaching by luminescence in vitro by recombination of radicals from polyunsaturated fatty acids. Free radic. Biol. Med. 53, 482. https://doi.org/10.1016/j.freeradbiomed.2012.05.030.

Narici, L., Paci, M., Brunetti, V., Rinaldi, A., Sannita, W.G., Carozzo, S., DeMartino, A., 2013. Bovine rod rhodopsin: 2. Bleaching in vitro upon ^{12}C ions irradiation as source of effects as light flash for patients and for humans in space. Int. J. Radiat. Biol. 89 (10), 765–769. https://doi.org/10.3109/09553002.2013.800245.

Narici, L., Titova, E., Obenaus, A., Wroe, A., Loredo, L., Schulte, R., Slater, J.D., Nelson, G.A., 2020. Multiple sensory illusions are evoked during the course of proton therapy. Life Sci. Space Res. 26. https://doi.org/10.1016/j.lssr.2020.04.006.

Narici, L., 2024. Light flashes and other sensory illusions perceived in space travel and on ground, including proton and heavy ion therapies. Z Med. Phys. 34, 1. https://doi.org/10.1016/j.zemedi.2023.06.004.

Pinsky, L.S., Osborne, W.Z., Bailey, J.V., Benson, R.E., Thompson, L.F., 1974. Light flashes observed by astronauts on Apollo 11 through Apollo 17. Science 183 (4128). https://doi.org/10.1126/science.183.4128.957.

Pinto, M., Pimpinella, M., Quini, M., D'Arienzo, M., Astefanoaei, I., Loreti, S., Guerra, A. S., 2016. A graphite calorimeter for absolute measurements of absorbed dose to water: application in medium-energy x-ray filtered beams. Phys. Medi. Biol. 61, 1738–1764. https://doi.org/10.1088/0031-9155/61/4/1738.

Power, A.S., Ward, M.L, 2025. Measurement of intracellular Ca^{2+} in muscle isolated from rat and Human hearts. Methods Mol Biol 2894. https://doi.org/10.1007/978-1-0716-4342-6_7.

Qin, G., Zhang, P., Sun, M., Fu, W., Cai, C., 2022. Comprehensive spectral libraries for various rabbit eye tissue proteomes (2022). Sci. Data 9, 111. https://doi.org/10.1038/s41597-022-01241-5.

Sannita, W.G., Peachey, N.S., Strettoi, E., Ball, S.L., Belli, F., Bidoli, V., Carozzo, S., Casolino, M., Di Fino, L., Picozza, P., Pignatelli, V., Rinaldi, A., Saturno, M., Schardt, D., Vazquez, M., Zaconte, V., Narici, L., 2007. Electrophysiological responses of the mouse retina to 12C ions. Neurosci. Lett. 416, 3. https://doi.org/10.1016/j.neulet.2006.12.062.

Schardt, D., Krämer, M., 2002. Particle induced visual sensations in heavy-ion tumor therapy. GSI Report, Vol. 2002-1 (GSI, Darmstadt). Wissenschaftlicher Ergebnisbericht der GSI, GSI Annual Report.

Schardt, D., Kavatsyuk, O., Krämer, M., Durante, M., 2013. Light flashes in cancer patients treated with heavy ions. Brain Stimul 6, 3. https://doi.org/10.1016/j.brs.2012.08.003.

Valiente-Gabioud, A.A., Garteizgogeascoa Suñer, I., Idziak, A., Fabritius, A., Basquin, G., Angibaud, J., Nägerl, U.V., Singh, S.P., Griesbeck, O., 2023. Fluorescent sensors for imaging of interstitial calcium. Nat. Commun. 14, 6220.

Zou, J., Hofer, A.M., Lurtz, M.M., Gadda, G., Ellis, A.L., Chen, N., Huang, Y., Holder, A., Ye, Y., Louis, C.F., Welshhans, K., Rehder, V., Yang, J.J., 2007. Developing sensors for real-time measurement of high Ca^{2+} concentrations. Biochemistry 46. https://doi.org/10.1021/bi7007307.